J. Cosmet. Sci., **70,** 149–159 (May/June 2019)

Facile Synthesis of Titanium Phosphates from Ilmenite Mineral Sand: Potential White Pigments for Cosmetic Applications

LALINDA PALLIYAGURU, M. USHAN S. KULATHUNGA, K. G. UPUL R. KUMARASINGHE, CHAMPA D. JAYAWEERA, and PRADEEP M. JAYAWEERA*, *Department of Chemistry, University of Sri Jayewardenepura, Nugegoda, Sri Lanka (L.P., M.U.S.K., K.G.U.R.K., C.D.J., P.M.J.)*

Accepted for publication June 8, 2019.

Synopsis

Ilmenite mineral sand was used to synthesize titanium bismonohydrogen orthophosphate monohydrate, $Ti(HPO_4)_2{\cdot}H_2O$, and titanium phosphate, TiP_2O_7, two white pigments suitable in cosmetic applications. $Ti(HPO_4)_2{\cdot}H_2O$ was obtained after digesting ilmenite in 85% phosphoric acid at 150 °C for 5 hours. On standing, unreacted ilmenite and white $Ti(HPO_4)_2{\cdot}H_2O$ solid separated into two layers and $Ti(HPO_4)_2{\cdot}H_2O$ was calcined at 900 °C to obtain the crystalline TiP_2O_7. Chemical and morphological characteristics were investigated using X-ray diffraction, transmission electron microscopy, scanning electron microscopy coupled with energy dispersive X-ray analysis, Fourier-transform infrared, and X-ray photoelectron spectroscopic techniques. The water retention (WR) capacities were measured at a relative humidity of 57% and indicate that $Ti(HPO_4)_2{\cdot}H_2O$ and TiP_2O_7 have increased WR ability when compared with the pigment grade (PG) TiO_2. The optical properties of $Ti(HPO_4)_2{\cdot}H_2O$, TiP_2O_7, and PG-TiO_2 were compared using Ultraviolet-visible diffuse reflectance spectroscopy. The relative photoactivity of $Ti(HPO_4)_2{\cdot}H_2O$ and TiP_2O_7 was determined using a chemical method based on the photobleaching behavior of a stable radical, 1,1-diphenyl 2-picrylhydrazyl. The photoactivities of $Ti(HPO_4)_2{\cdot}H_2O$ and TiP_2O_7 are lower than that of PG-TiO_2.

INTRODUCTION

Pigment-grade (PG) titanium dioxide (TiO_2) has a number of applications in the cosmetic industry (1–3). Skin care products that use PG-TiO_2 have several disadvantages, e.g., certain degree of photocatalytic breakdown of sebum which provides lubrication and protection to the skin from infections (4,5). In addition, it has been reported that nanoscale TiO_2 could penetrate into the body through the skin, causing health risks (6,7). Mixing of silicon dioxide (SiO_2) with PG-TiO_2 has been recently investigated in view of minimizing the sebum breakdown and absorption through the skin (6). Application of SiO_2-TiO_2 composite in cosmetics has been severely hampered by the hardness of the composite

Address all correspondence to P. M. Jayaweera at pradeep@sjp.ac.lk.

compared with PG-TiO_2. This opens up an opportunity for a new substitute to replace the PG-TiO_2 or TiO_2-SiO_2 in the cosmetic industry. Titanium phosphates (TPs) are gentle white powders and weakly photoactive (8,9). Therefore, TPs are potential candidates for replacing PG-TiO_2 or TiO_2-SiO_2. Usually, TPs are synthesized using titanium compounds, such as titanium chloride and sulfate (10–13). The decomposition of sphene, $CaTiOSiO_4$, by H_3PO_4 has also been successfully used to synthesize TPs (14).

The direct use of a natural material to synthesize TPs has environmental and economic advantages. The common natural titanium-rich minerals used in the TiO_2 manufacturing process are rutile, ilmenite, and leucoxene (15). Ilmenite ($FeTiO_3$) is currently the most common feedstock because many rutile deposits are becoming depleted through commercial use (16,17).

The present investigation reveals a simple, low-cost method to synthesize titanium bismonohydrogen orthophosphate monohydrate (TOP) and TP with the chemical formulae of $Ti(HPO_4)_2{\cdot}H_2O$ and TiP_2O_7 respectively, using a natural starting material of ilmenite mineral sand. The optical properties, the water retention (WR) capacities, and the photoactivities of the synthesized TPs were compared with PG-TiO_2 to assess the suitability of these materials for the cosmetic industry.

EXPERIMENTAL SECTION

In a typical experiment, TOP, i.e., $Ti(HPO_4)_2{\cdot}H_2O$ was synthesized by digesting 100 g of ilmenite (Lanka Mineral Sands Limited, Rajagiriya, Sri Lanka) and 400 mL of 85% H_3PO_4 (Daejung Chemicals, Siheung-si, South Korea) for 5 h with vigorous stirring at 150 °C. The reaction mixture was allowed to cool and settle down at room temperature. Dense unreacted ilmenite (gray black color) settled down to the bottom of the vessel rapidly, whereas less dense solid TOP (white color) slowly settled as two very distinct solid layers (Figure 1). Leachate was carefully decanted and the solid TOP layer was separated out from the unreacted ilmenite and thoroughly washed with distilled water several times to remove any trace acid. TOP was dried at 80 °C and stored in a desiccator for further use. The resulted TOP was converted to TP by calcining (box-type resistance furnace SX-2.5-10, Zhejiang Top Cloud-Agri Technology Co. Ltd, Zhejiang, China) at 900 °C for 4 h.

X-ray diffraction (XRD) patterns of ilmenite and the synthesized TPs were analyzed using XRD instrument (Rigaku Ultima-IV, Rigaku, Tokyo, Japan) equipped with Cu Kα source and scintillation detector. The morphology of the powder materials were investigated by the high-resolution transmission electron microscopy (HR-TEM ZEISS Libra 200 Cs-TEM, Carl Zeiss AG, Oberkochen, Germany) at an accelerating voltage of 200 kV. An energy-dispersive X-ray (EDX) analysis coupled with (scanning electron microscopy, Zeiss EVO 18, Carl Zeiss AG) microscope was also used to obtain the elemental identification of the samples.

X-ray photoelectron spectroscopic (XPS) analyses were carried out with Axis Ultra DLD spectrometer (Kratos, Kratos Analytical Ltd, Manchester, UK) using a monochromatic Al Kα source. Instrument base pressure was 8×10^{-10} Torr. The XPS spectra were collected using an analysis area of ~300×700 μm. The pass energy of 160 and 20 eV were used for wide and narrow spectra, respectively. The charge neutralizer system was used for all analyses. Curve fitting of raw data was performed using XPS Peak Fit software Version 4.1

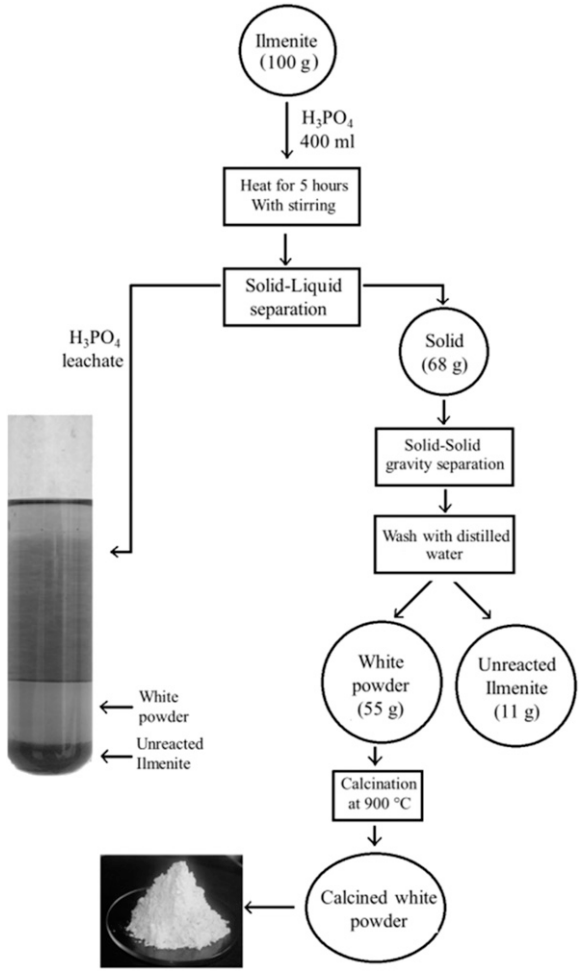

Figure 1. The flowchart of TOP and TP preparation process.

(Morton, S. 1995–2006, Casa Software Ltd, Teignmouth, UK) with a Lorentzian/Gaussian percentage as 40 and a Shirley background. Fourier-transform infrared (FTIR) data were acquired using Thermo Scientific Nicolet iS10 FT-IR spectrometer (Thermo Fisher Scientific, Waltham, MA).

The WR capacities of synthesized pigments were tested by mixing a sample of 1.9 g of pigment material with 0.1 g of urea and 1.3 g of distilled water. The thoroughly mixed paste was spread on a glass plate to make a thin layer, and weight loss was measured using an analytical balance (Precisa XT 220A, Precica Gravimetric AG, Dietikon, Switzerland) at 26°C and at a relative humidity of 57%. The weight loss of the samples was recorded hourly for 7 h. PG-TiO_2 (Brand Ti-Pure™, Chemours, Wilmington, DE) and Degusa P25 (Nippon Aerosil Co., Ltd., Tokyo, Japan) were used as the control. Percentage WR was calculated using the following equation: $WR\% = \left\{\frac{\left[w_0 - \left(w_1 - w_t\right)\right]}{w_0}\right\} \times 100$ where,

w_0 = weight of the water, w_1 = initial weight of the moist sample with water, and w_t = weight of the moist sample at different time intervals (18,19).

UV-Vis diffuse reflectance spectra (UV-Vis DRS) of the powder samples of TOP, TP, PG-TiO_2, and Degussa P25 were measured using a PerkinElmer Lambda 35 spectrometer (Perkin-Elmer Inc., Waltham, MA). UV-Vis DRS were obtained with 1.25-inch calibrated certified reflectance standard (Spectralon Diffuse Reflectance Standard-99-010) as the background equipped with a 50 mm integrating sphere. The optical absorbance was measured in the 300–900 nm range.

The photoactivities of synthesized TOP and TP were compared with both PG-TiO_2 and Degussa P25 by measuring the photoreduction of 2,2-diphenyl-1-picrylhydrazyl radical (DPPH) (20). In a typical experiment, 20 mg of the sample was dispersed in a solution of DPPH (Sigma-Aldrich, Taufkichen, Germany) in a 1:1 mixture $\left(2\times10^{-4}\ \text{mol dm}^{-3}\right)$ of mineral oil and caprylic/capric acid triglyceride (Sigma-Aldrich) and irradiated using a 250 W Hg arc Philips UV lamp. Control experiments were performed under dark condition for comparison. Freshly prepared DPPH solutions were used in each experiment. The time dependence of DPPH radical scavenging was tested by withdrawing samples out of the reaction mixture every 10 min and measuring the absorbance at 520 nm (Perkin-Elmer Lambda 35, Perkin-Elmer Inc.).

RESULTS AND DISCUSSION

CHEMICAL CHARACTERIZATION AND THE MORPHOLOGY OF THE TPS

A gradual formation of a gray color mixture was observed as the leaching of ions from ilmenite into H_3PO_4 solution take place at 150 °C for 5 h. When the mixture was allowed to settle at room temperature, a white precipitate separated from unreacted ilmenite and H_3PO_4 leachate (Figure 1). The two solid phases can be easily separated with a ~55% yield of the white precipitate. The unreacted ilmenite (~11%) and the H_3PO_4 liquor can be used for further use.

The XRD patterns of the ilmenite and TOP are shown in Figure 2A and B, respectively (21). Figure 2B confirms the microstructure of TOP with the chemical formula of $Ti(HPO_4)_2{\cdot}H_2O$, (ICDD-01-080-1067) (22,23). The XRD pattern of TP obtained after calcining TOP at 900°C for 4 h is shown in Figure 2C. The conversion of TOP to TP phase was confirmed by the XRD data. Figure 2C is matched with the XRD pattern of TP with the chemical formula of TiP_2O_7 (ICDD-01-082-3834) (24). The calcination of TOP to TP proceeds with the removal of water from TOP. The appearance of additional peaks for the TP in the XRD at higher 2θ confirms the crystallinity of the powdered sample of TP (25). Furthermore, the XRD pattern of ilmenite is significantly different from the XRD patterns of TOP and TP, confirming the formation of new compounds during the acid digestion. The absence of any XRD peaks corresponding to iron-bearing compounds suggests that both TOP and TP are relatively free from iron.

The TEM images of synthesized TPs are shown in Figure 3. The TEM images confirm the presence of spherical shaped particles for both TOP and TP with an average diameter of 75 and 115 nm, respectively. The EDX analysis data of the prepared TPs are shown in Figure 3. The occurrence of intense peaks corresponding to O, P, and Ti in both EDX spectra confirms that TOP and TP largely contain phosphate forms of titanium. The presence of a small

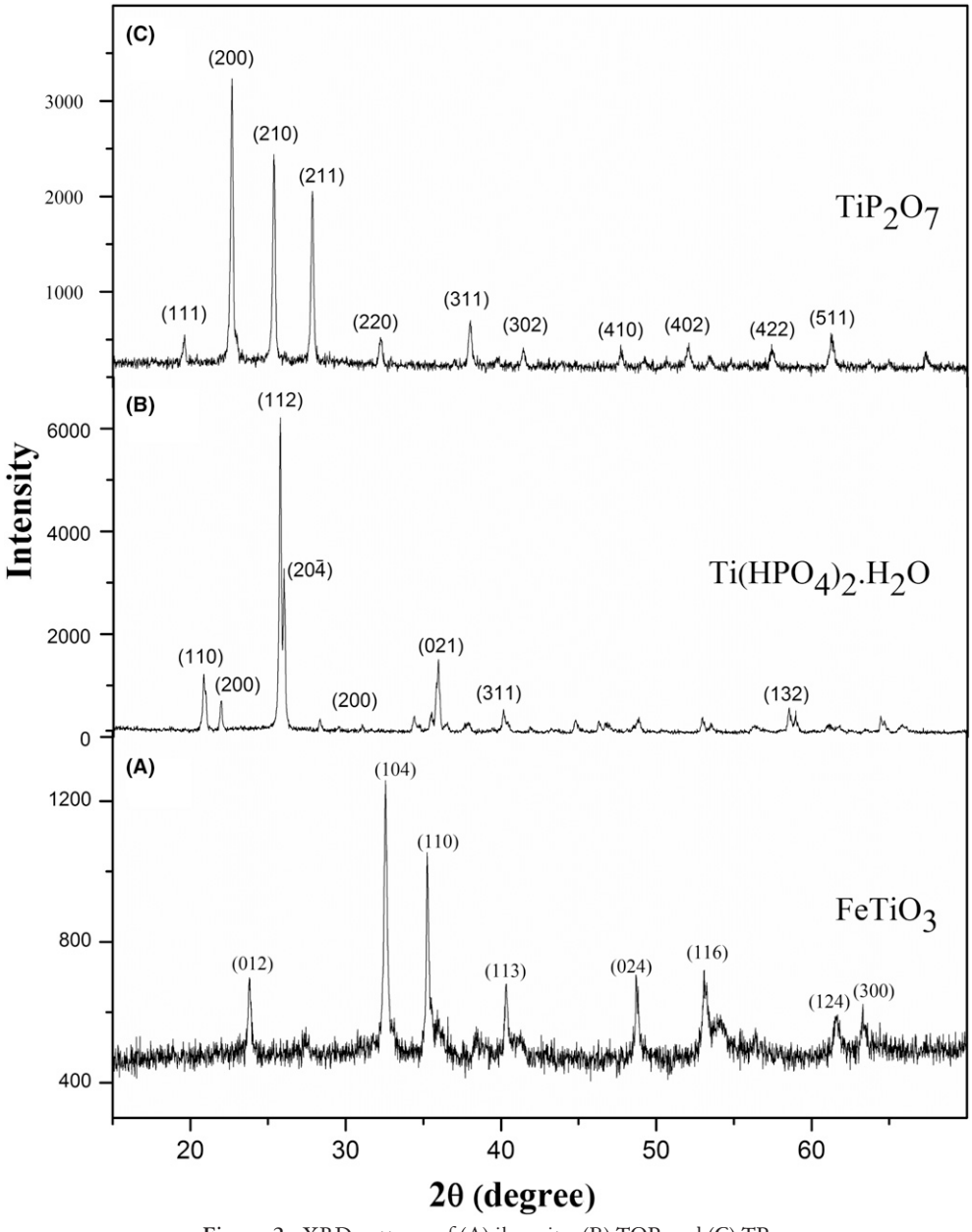

Figure 2. XRD patterns of (A) ilmenite, (B) TOP, and (C) TP.

amount of iron (<5% w/w) in TOP and TP is evident by the weak peaks appearing at 6.4 and 7.5 keV regions in EDX spectra. The removal of coprecipitated iron, a common impurity, is difficult and is a costly process in the production of TiO_2 (26). However, the results in the present study clearly indicate that leaching of iron from ilmenite in concentrated H_3PO_4 is less problematic as a result of the formation of multiligand complexes such as $Fe(H_2PO_4)^{2+}$, $FeH_5(PO_4)_2^{2+}$, and $FeH_7(PO_4)^{3+}$, which are highly soluble (27).

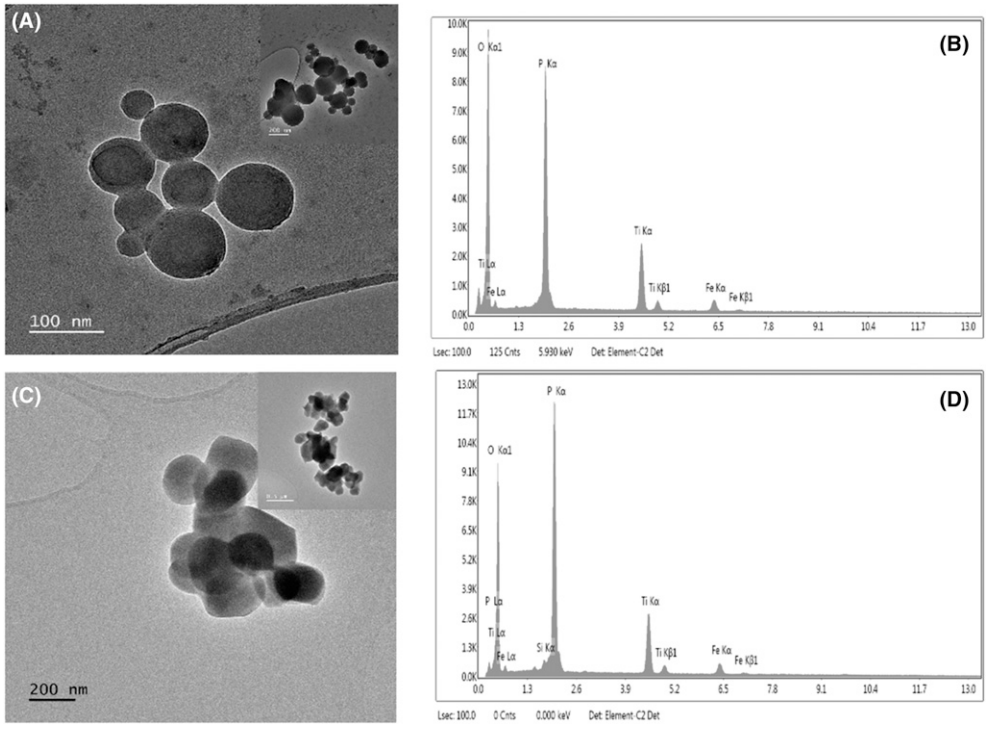

Figure 3. TEM images and EDX analysis: (A), (B) for TOP and (C), (D) for TP.

XPS scans (see supplementary material) of ilmenite and TPs show the characteristic Ti2p peak appearing at 459.3 eV. However, peak fitting confirms the presence of two peaks for natural ilmenite, indicating two different oxidation states for the titanium atoms. The asymmetrically broad $Ti2p_{3/2}$ photoelectron peak suggests the presence of both +3 and +4 oxidation states for titanium. The two peaks observed for the $Ti2p_{3/2}$ appear at 458.1 and 459.3 eV. The Ti2p and Fe2p XPS data suggest that natural weathered ilmenite used in this work contain Ti and Fe atoms in their two common oxidations states, Fe^{2+}/Ti^{4+} and Fe^{3+}/Ti^{3+}. The appearance of an intense P2p peak at 134.3 eV and the absence of Fe2p peak in the iron region for the XPS scan of TOP clearly suggest that ilmenite has converted into TOP during acid digestion with low iron content.

FTIR spectra of TPs show the characteristic overlapped bands in the 960–1200 cm^{-1} range because of antisymmetric P–O stretching vibration. The relevant bending vibrations appear at lower frequencies less than 670 cm^{-1}. Based on the previously published data, it can be suggested that the phosphate ions form the ideal tetrahedral structures for the TPs (see supplementary material) (28,29).

The white powder obtained with a low iron content from digestion of ilmenite in H_3PO_4 is $Ti(HPO_4)_2{\cdot}H_2O$ and calcination has led to the production of TiP_2O_7. Results clearly confirm the chemical identity and the morphology of synthesized $Ti(HPO_4)_2{\cdot}H_2O$ and TiP_2O_7. Furthermore, XRF analysis (see supplementary material) of TOP and TP indicate the high purity of synthesized materials with trace amounts of other metals.

COSMETIC PROPERTIES OF SYNTHESIZED TPs

UV-Vis DRS (Figure 4) were obtained to assess the optical property of synthesized samples of TPs and to compare with PG-TiO_2 and Degussa P25. The degree of diffuse reflectance is dependent on parameters such as the refractive index, band gap, shape, and particle size of the material. A higher refractive index of 2.6 for TiO_2 (30) favors higher light scattering properties than TPs, which has a lower refractive index below 1.8 (31). Therefore, Degussa P25 (Figure 4C) and PG-TiO_2 (Figure 4D) show comparatively higher diffuse reflectance than TPs (Figure 4A and B). PG-TiO_2 having particle diameter >50 nm exhibit lower diffuse reflectance than Degussa P25.

The pigment materials used in cosmetic products having a lower photoactivity is an added advantage to minimize a certain degree of sebum breakdown on the skin (6,7). Titanium dioxide, the white pigment used in cosmetics is a powerful photoactive material capable of degrading wide variety of organic substances via rapid photochemical reactions in hydrated environments (32–34). Therefore, photoactivity of the synthesized TOP and TP were tested and compared with both PG-TiO_2 and Degussa P25. Photo-induced abstraction of hydrogen atoms from hydrocarbons by DPPH can be assisted by the presence of semiconductor materials such as TiO_2 (35,36). Photo-induced fading of DPPH from purple to pale yellow was followed by a rapid decrease in the absorption at 520 nm (see Figure 5B). The photoactivities of TP, TOP, PG-TiO_2, and Degussa 25 were compared by measuring the decrease in absorption intensity at 520 nm for a period of 30 min of the analyte containing DPPH mixture and a test material. Gradual decrease in the

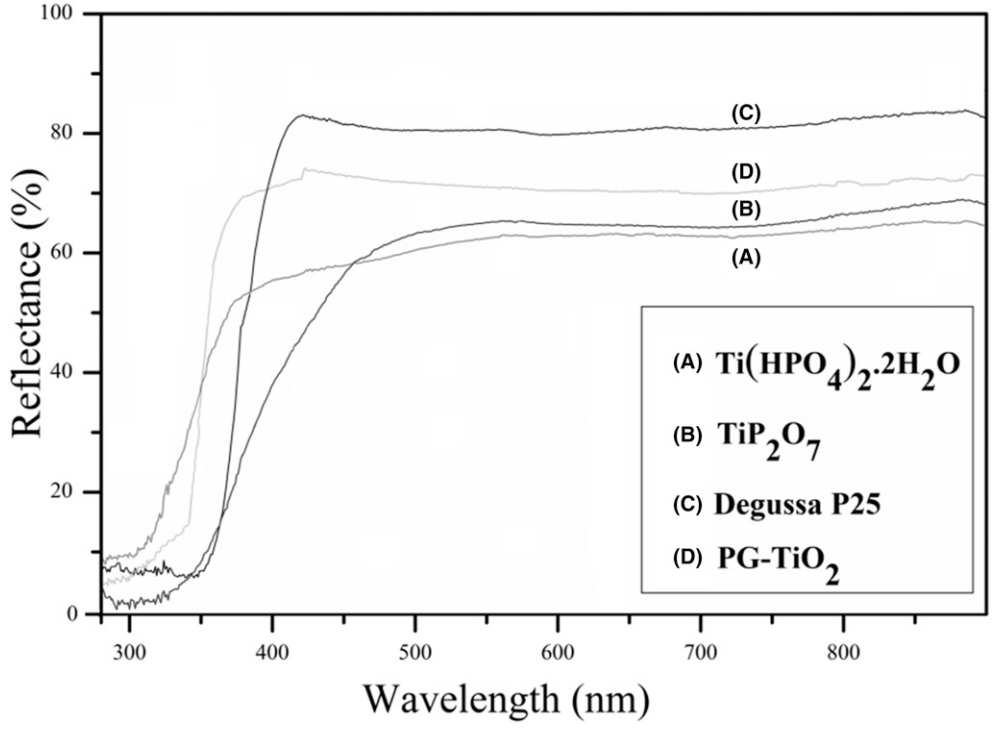

Figure 4. UV-Vis DRS of (A) TOP, (B) TP, (C) P25, and (D) PG-TiO_2.

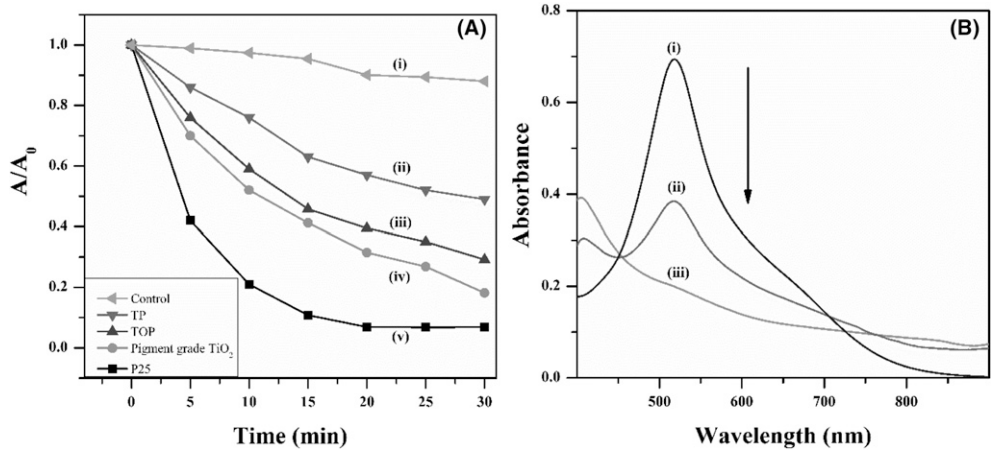

Figure 5. (A) Effect of UV irradiation on DPPH absorption at 520 nm with (i) no catalyst, (ii) TP, (iii) TOP, (iv) PG-TiO_2, and (v) Degussa P25 dispersions. (B) UV-Vis absorption spectra of the $DPPH^{\bullet}$ radical (i) and (ii-iii) the reduced form of the $DPPH_2$.

peak intensity at 520 nm recorded as a function of time is shown in Figure 5A. Samples show a 50% drop of the intensity at 28, 13, 11, and 4 min, respectively, for TP, TOP, PG-TiO_2, and Degussa P25. Results clearly indicate that synthesized TP and TOP are fairly photoinactive when compared with TiO_2.

WR ability is another significant parameter in cosmetic products and urea is commonly used as an additive to maintain the moisture level on the skin and for the smoothness (37). Therefore, WR capacities of both TOP and TP samples with 5% w/w urea were tested after moisturizing at 57% RH (Figure 6A and B) (18). PG-TiO_2 and Degussa P25 TiO_2 were used as controls (Figure 6C and D). For TOP, PG-TiO_2, and Degussa P25 TiO_2, WR capacities rapidly declined to a 15–20% level because of the evaporation of loosely bound water from the surface in the first 5 h. Subsequently, it remained relatively constant for the next tested time period. Interestingly, TP indicates a drop of WR to ~35% at 5 h and thereafter shows a slow water release rate. After 7 h, it shows about ~30% WR capacity, a higher value than TOP and control TiO_2 samples. This indicates a good WR ability for the synthesized TP, which is better than the commercially available TiO_2.

CONCLUSIONS

Two potential replacements for PG-TiO_2 in cosmetic products, TOP and TP, were synthesized using ilmenite obtained from mineral sand as the starting material through H_3PO_4 digestion. The synthesized TOP and TP white pigments demonstrate significantly less photoactivity than PG-TiO_2, implying a reduced risk of sebum breakdown on human skin. The WR capacities of moisturized pastes prepared with powdered materials, TOP, TP, and TiO_2 with 5% urea, were measured. The synthesized TP shows a better WR capacity than TOP and PG-TiO_2. As a potential next step in this research, safety data would be needed to generate to be used as a permitted colorant in the cosmetics industry.

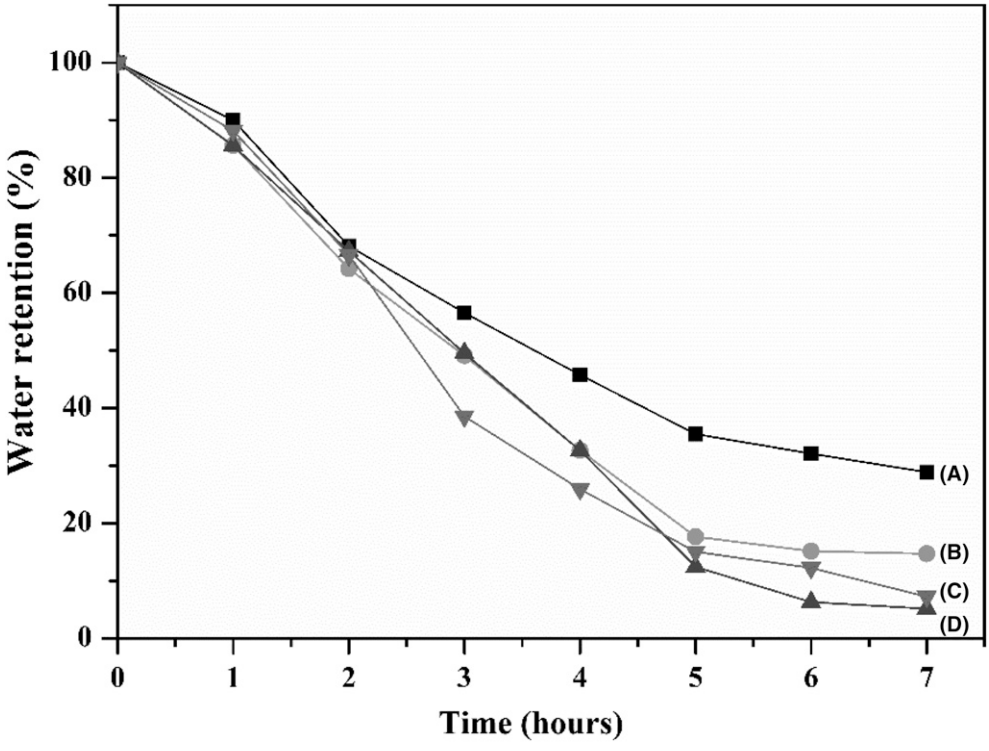

Figure 6. Percentage WR capacities at 57% relative humidity for (A) TP, (B) TOP, (C) PG-TiO_2, and (D) Degussa P25 with 5% (w/w) urea.

ACKNOWLEDGMENTS

The authors thank Lanka Mineral Sands Ltd., Sri Lanka, for providing ilmenite samples; Dr. Asitha Cooray, Central Instrument Facility, University of Sri Jayewardenepura, for XRD sample analysis; Prof. Masaru Shimomura, Department of Electronics and Materials Science, Graduate School of Integrated Science and Technology, Shizuoka University for XPS studies; and University of Sri Jayewardenepura for the research grant ASP/01/RE/SCI/2018/14.

REFERENCES

(1) A. Weir, P. Westerhoff, L. Fabricius, K. Hristovski, and N. von Goetz, Titanium dioxide nanoparticles in food and personal care products, *Environ. Sci. Technol.*, **46**, 2242–2250 (2012).
(2) M. Auffan, M. Pedeutour, J. Rose, A. Masion, F. Ziarelli, D. Borschneck, C. Chaneac, C. Botta, P. Chaurand, J. Labille, and J.-Y. Bottero, Structural degradation at the surface of a TiO_2-based nanomaterial used in cosmetics, *Environ. Sci. Technol.*, 44, 2689–2694 (2010).
(3) G. P. Dransfield, Inorganic sunscreens, *Radiat. Protect. Dosim.*, **91**, 271–273 (2000).
(4) M. Picardo, M. Ottaviani, E. Camera, and A. Mastrofrancesco, Sebaceous gland lipids, *Dermato-endocrinology*, 1, 68–71 (2009).
(5) H. J. Choi, K.-C. Park, H. Lee, T. Crouzier, M. F. Rubner, R. E. Cohen, G. Barbastathis, and G. H. McKinleyand, Superoleophilic titania nanoparticle coatings with fast fingerprint decomposition and high transparency, *ACS Appl. Mater. Interfaces*, **9**, 8354–8360 (2017).

(6) M. Senzui, T. Tamura, K. Miura, Y. Ikarashi, Y. Watanabe, and M. Fujii, Study on penetration of titanium dioxide (TiO(2)) nanoparticles into intact and damaged skin in vitro, *J. Toxicol. Sci.*, **35**, 107–113 (2010).
(7) J. Wu, W. Liu, C. Xue, S. Zhou, F. Lan, L. Bi, H. Xu, X. Yang, and F. D. Zeng, Toxicity and penetration of TiO_2 nanoparticles in hairless mice and porcine skin after subchronic dermal exposure, *Toxicol. Lett.*, **191**, 1–8 (2009).
(8) F.-F. Cheng, T.-T. He, H.-T. Miao, J.-J. Shi, L.-P. Jiang, and J.-J. Zhu, Electron transfer mediated electrochemical biosensor for microRNAs detection based on metal ion functionalized titanium phosphate nanospheres at attomole level, *ACS Appl. Mater. Interfaces.*, **7**, 2979–2985 (2015).
(9) M. Yada, Y. Inoue, A. Sakamoto, T. Torikai, and T. Watari, Synthesis and controllable wettability of micro- and nanostructured titanium phosphate thin films formed on titanium plates, *ACS Appl. Mater. Interfaces*, **6**, 7695–7704 (2014).
(10) G. Alberti, P. Cardini-Galli, U. Costantino, and E. Torracca, Crystalline insoluble salts of polybasic metals-I ion-exchange properties of crystalline titanium phosphate, *J. Inorg. Nucl. Chem.*, **29**, 571–578 (1967).
(11) A. Bhaumik and S. Inagaki, Mesoporous titanium phosphate molecular sieves with ion-exchange capacity, *J. Am. Chem. Soc.*, **123**, 691–696 (2001).
(12) H. Onoda, S. Fujikado, and T. Toyama, Preparation of titanium phosphate white pigments with titanium sulfate and their powder properties, *J. Adv. Ceram.*, **3**, 132–136 (2014).
(13) A. Bortun, E. Jaimez, R. Llavona, J. García, and J. Rodríguez, Formation of crystalline titanium(IV) phosphates from titanium(III) solutions, *Mater. Res. Bull.*, **30**, 413–420 (1995).
(14) M. Maslova, D. Rusanova, V. Naydenov, O. Antzutkin, and L. G. Gerasimova, Formation of titanium phosphate composites during phosphoric acid decomposition of natural sphene, *J. Solid State Chem.*, **181**, 3357–3365 (2008).
(15) K. K. Sahu, T. C. Alex, D. Mishra, and A. Agrawal, An overview on the production of pigment grade titania from titania-rich slag, *Waste Manag. Res.*, **24**, 74–79 (2006).
(16) S. Zhang and M. J. Nicol, An electrochemical study of the reduction and dissolution of ilmenite in sulfuric acid solutions, *Hydrometallurgy*, **97**, 146–152 (2009).
(17) L. Palliyaguru, N. D. H. Arachchi, C. D. Jayaweera, and P. M. Jayaweera, Production of synthetic rutile from ilmenite via anion-exchange, *Miner. Procss. Extr. Metall.*, **127**, 169–175 (2017).
(18) H. He, R. Cai, Y. Wang, G. Tao, P. Guo, H. Zuo, L. Chen, X. Liu, P. Zhao, and Q. Xia, Preparation and characterization of silk sericin/PVA blend film with silver nanoparticles for potential antimicrobial application, *Int. J. Biol. Macromol.*, **104**, 457–464 (2017).
(19) A. Lateef, R. Nazir, N. Jamil, S. Alam, R. Shah, M. N. Khan, and M. Saleeme, Synthesis and characterization of zeolite based nano-composite: anenvironment friendly slow release fertilizer, *Microporous Mesoporous Mater.*, **232**, 174–183 (2016).
(20) G. Dransfield, P. J. Guest, P. L. Lyth, D. J. McGarvey, and T. G. Truscott, Photoactivity tests of TiO_2-based inorganic sunscreens. Part 1: non-aqueous dispersions, *J. Photochem. Photobiol. B Biol.*, **59**, 147–151 (2000).
(21) N. D. H. Arachchi, G. S. Peiris, M. Shimomura, and P. M. Jayaweera, Decomposition of ilmenite by ZnO/ZnS: enhanced leaching in acid solutions, *Hydrometallurgy*, **166**, 73–79 (2016).
(22) X. Wang, X. Yang, J. Cai, T. Miao, L. Li, G. Li, D. Deng, L. Jiang, and C. Wang, Novel flower-like titanium phosphate microstructures and their application in lead ion removal from drinking water, *J. Mater. Chem. A*, **2**, 6718–6722 (2014).
(23) H. B. Ortíz-Oliveros, R. M. Flores-Espinosa, E. Ordoñez-Regil, and S. M. Fernández-Valverde, Synthesis of α-$Ti(HPO_4)_2{\cdot}H_2O$ and sorption of Eu(III), *Chem. Eng. J.*, **236**, 398–405 (2014).
(24) Y. N. Wang and J. J. Bian, Effects of P_2O_5/TiO_2 ratio on the sintering behavior and microwave dielectric properties of TiP_2O_7, *Ceram. Int.*, **41**, 4683–4687 (2015).
(25) H. Onoda and T. Yamaguchi, Influence of ultrasonic treatment on preparation and powder properties of titanium phosphates, *J. Mater. Chem.*, **22**, 19826–19830 (2012).
(26) D. Filippou and G. Hudon, Iron removal and recovery in the titanium dioxide feedstock and pigment industries, *JOM*, **61**, 36 (2009).
(27) T. Zhang, Y. Lu, and G. Luo, Effects of temperature and phosphoric acid addition on the solubility of iron phosphate dihydrate in aqueous solutions, *Chin. J. Chem. Eng.*, **25**, 211–215 (2017).
(28) A. Stoch, W. Jastrzębski, A. Brożek, J. Stoch, J. Szaraniec, B. Trybalska, and G. Kmitaa, FTIR absorption–reflection study of biomimetic growth of phosphates on titanium implants, *J. Mol. Struct.*, **555**, 375–382 (2000).
(29) T. S. Sysoeva, E. A. Asabina, V. I. Pet'kov, and V. S. Kurazhkovskaya, Alkali (alkaline-earth) metal, aluminum, and titanium complex orthophosphates: synthesis and characterization, *Russ. J. Inorg. Chem.*, **54**, 829–839 (2009).

(30) S. R. Pinnell, D. Fairhurst, R. Gillies, M. A. Mitchnick, and N. Kollias, Microfine zinc oxide is a superior sunscreen ingredient to microfine titanium dioxide, *Dermatol. Surg.*, **26**, 309–314 (2000).
(31) T. Dobbelaere, F. Mattelaer, J. Dendooven, P. M. Vereecken, and C. Detavernier, Plasma-enhanced atomic layer deposition of iron and titanium phosphates as electrode materials for 3D-structured lithium-ion microbatteries, *ECS Trans.*, **75**, 35–44 (2016).
(32) T. Ohno, K. Sarukawa, K. Tokieda, and M. Matsumura, Morphology of a TiO_2 photocatalyst (Degussa, P-25) consisting of anatase and rutile crystalline phases, *J. Catal.*, **203**, 82–86 (2001).
(33) A. R. Khataee and M. B. Kasiri, Photocatalytic degradation of organic dyes in the presence of nanostructured titanium dioxide: influence of the chemical structure of dyes, *J. Mol. Catal. A Chem.*, **328**, 8–26 (2010).
(34) S. Lakshmi, R. Renganathan, and S. Fujita, Study on TiO_2-mediated photocatalytic degradation of methylene blue, *J. Photochem. Photobiol. A.*, **88**, 163–167 (1995).
(35) J. N. Pitts, E. A. Schuck, and J. K. S. Wan, Photoreduction of 2,2-diphenyl-1-picrylhydrazyl (DPPH) in hydrocarbons, *J. Am. Chem. Soc.*, **86**, 296–297 (1964).
(36) T. A. Egerton and J. A. Mattinson, Comparison of photooxidation and photoreduction reactions on TiO_2 nanoparticles, *J. Photochem. Photobiol. A.*, **186**, 115–120 (2007).
(37) S. Purnamawati, N. Indrastuti, R. Danarti, and T. Saefudin, The role of moisturizers in addressing various kinds of dermatitis: a review, *Clin. Med. Res.*, **15**, 75–87 (2017).